

# ASSESSMENT OF IN-SITU TESTS FOR STIFFNESS AND STRENGTH CHARACTERISTICS OF PAVEMENT MATERIALS

**Yongyuth Taesiri**  
**Auckpath Sawangsuriya**  
*Bureau of Road Research and Development*  
*Department of Highways, Thailand*  
sawangsuria@gmail.com

**Suppakorn Wachiraporn**  
*Bureau of Highway Construction 1*  
*Department of Highways, Thailand*  
wachiraporn08@gmail.com

**Wilailak Sramoon**  
*Department of Civil Engineering*  
*Mahanakorn University of Technology, Thailand*  
wilailakk@gmail.com

## ABSTRACT

Given the importance of the mechanical or structural properties (i.e., stiffness and strength) in pavement materials evaluation, there is a trend toward using methods for quantitative evaluations of these properties. In this paper, the soil stiffness gauge (SSG) and the dynamic cone penetrometer (DCP) were employed to assess respectively the in-situ stiffness and strength of pavement layer materials (i.e., crushed rock base, soil-aggregate subbase, sand embankment etc.) from three highway construction sites around the city of Bangkok, Thailand. The SSG and DCP data were examined statistically and empirical correlations for all materials tested were developed accordingly. The SSG stiffness and DCP penetration index were also correlated with the elastic modulus (E) and California bearing ratio (CBR) of the materials, respectively. The correlation data were also combined with those obtained from previous studies. A good correlation with a  $R^2$  value of 0.80 was obtained between E-value from the SSG and CBR from the DCP. Finally, elastic moduli from the SSG were compared with those from the falling weight deflectometer and the laboratory resilient modulus test. Similarly, CBR from the DCP was also compared with the conventional laboratory CBR test.

## 1. INTRODUCTION

To ensure that uniform and optimum improvement of pavement structure has been achieved, the quality of pavement and subgrade materials must be monitored during roadwork construction. Traditionally, quality control monitoring is achieved through moisture-density tests, visual inspection, observation of construction equipment, and proof rolling (i.e., passing a roller of a certain weight and measuring ensuing total or permanent deflections). In Thailand, the quality control evaluation during highway construction is typically based on in-place density measurement using the sand-cone method. All of these methods provide a measure of material quality index used to judge compaction acceptability but do not provide direct assessment of structural properties such as stiffness and strength. Furthermore, such methods do not ensure that a minimum stiffness or strength is achieved because different soils prepared at the same compaction density may have different stiffness and strength.

Direct monitoring of stiffness and strength is consistent with the transition from empirical to current mechanistic-empirical (M-E) pavement design procedures for structural design of flexible pavements. To successfully implement M-E pavement design procedure and to move toward performance-based specifications that are required to control the long-term functional and structural performance, additional in-situ stiffness and strength measurements should be included along with the conventional compaction control tests. Consequently, methods for in-situ stiffness and strength

assessment of compacted pavement materials must be portable, simple to use, reliable, reasonably accurate, instantaneous, and can be conducted independently and safely by the inspector without interference with the construction process.

A number of methods have been continuously developed and become currently available in the geotechnical and pavement engineering communities for direct measurement of in-situ stiffness and strength of pavement materials. These methods are portable, operator friendly, and also provide rapid and instantaneous measurement with reasonable accuracy during construction. Examples of these tools include the light weight deflectometer (LWD), the portable falling weight deflectometer (PFWD), the soil stiffness gauge (SSG), the Briard compaction device (BCD), the dynamic cone penetrometer (DCP) etc. [1] [2] [3] In this study, the SSG and the DCP will be implemented in three highway construction projects around the city of Bangkok, Thailand. The SSG and the DCP respectively offer a means of directly monitoring in-situ stiffness and index of strength of pavement materials. The SSG stiffness and DCP penetrometer index were also correlated to the elastic modulus and California bearing ratio, respectively. [2] The objectives of this study are: (1) to examine the use of the SSG and DCP for pavement materials evaluation in Thailand, (2) to explore the empirical correlations between the two devices, and (3) to compare the results with the other well-known or conventional tests.

## 2. SOIL STIFFNESS GAUGE (SSG)

The soil stiffness gauge (SSG), which is currently marketed as the Humboldt GeoGauge™ (Figure 1), is a portable, non-nuclear testing device that provides simple and non-destructive means of directly and rapidly measuring in-situ soil stiffness. The SSG weighs about 11.4 kg, is 28 cm in diameter, 25.4 cm height, and rests on the soil surface via a ring-shaped footing. The SSG measures near-surface stiffness by imparting small dynamic force to the soil through a ring-shaped foot at 25 steady state frequencies between 100 and 196 Hz. Based upon the force and displacement-time history, stiffness is calculated internally as the average force per unit displacement over the measured frequencies and reported. A measurement takes only about 1.5 minutes.

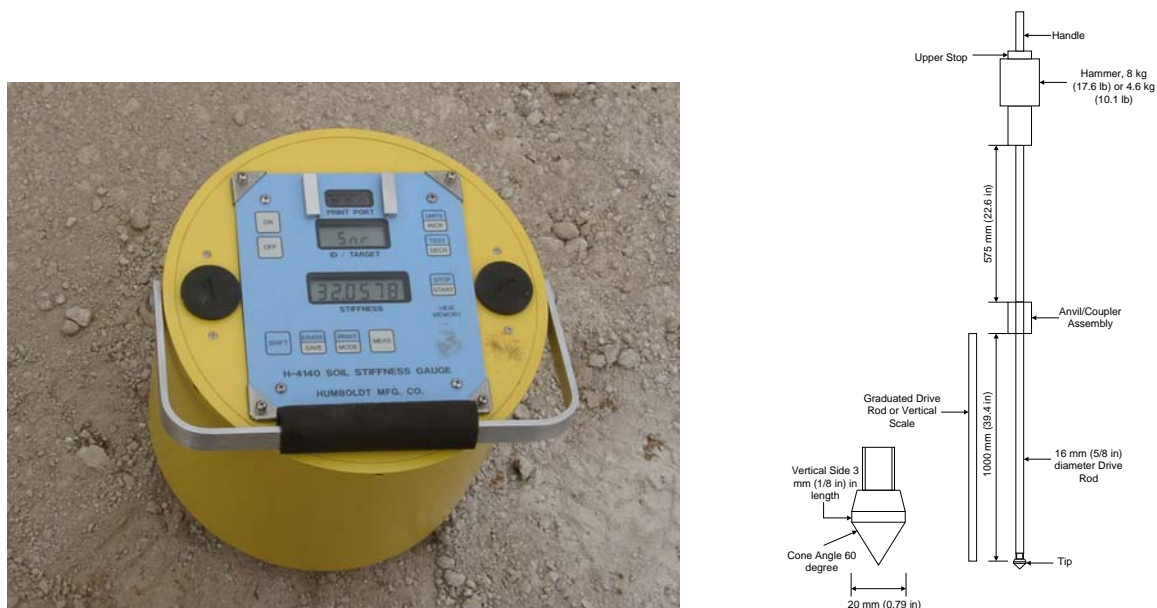


Figure 1 Soil stiffness gauge (Humboldt GeoGauge™) and dynamic cone penetrometer (DCP)

Sawangsurriya et al. [4] studied the zone of measurement influence and the effects of layered materials on the SSG measurement in granular materials. A finite-element analysis and the SSG measurements in a test box indicated that the radius of measurement influence extends to 300 mm. For two-layer materials with different stiffness, the SSG started to register the stiffness of an upper-layer material of 125 mm or thicker. The effect of the lower layer might continue to be present even at an upper-layer material thickness of 275 mm, depending on the relative stiffness (or contrast) of the layer materials. A comparison of moduli of granular soils obtained from the SSG with moduli obtained from other tests on the basis of comparable stress levels indicated that the SSG induced strain amplitudes were lower than the strain amplitudes induced in the resilient modulus test, however, larger than the strain amplitude of seismic test. [5]

The measured soil stiffness from the SSG can be used to calculate the modulus of the materials at near surface. For a rigid ring-shaped plate resting on a linear-elastic, homogeneous, and isotropic infinite half-space, the stiffness ( $K_{SSG}$ ) is related to modulus of soil ( $E_{SSG}$ ) [6]:

$$K_{SSG} = \frac{1.77E_{SSG}R}{(1-\nu^2)} \quad (1)$$

where  $\nu$  is Poisson's ratio of the materials and  $R$  is the outside radius of the ring (57.2 mm). Note that  $K_{SSG}$  and  $E_{SSG}$  are expressed in MN/m and MPa, respectively. Because of small strain amplitudes induced by the SSG, elastic response of the soils is assumed and the use of Eq. (1) is justified.

### 3. DYNAMIC CONE PENETROMETER (DCP)

The dynamic cone penetrometer (DCP) (Figure 1) is simple, rugged, economical, and able to provide a rapid in-situ index of strength of pavement structure. The DCP is used for measuring the material resistance to penetration in terms of millimetres per blow while the cone of the device is being driven into the pavement structure or the subgrade. The typical DCP consists of an 8-kg hammer that drops over a height of 575 mm, and drives a 60-degree 20-mm-base diameter cone tip vertically into the pavement structure or the subgrade. The steel rod to which the cone is attached has a smaller diameter than the cone (16 mm) to reduce skin friction. The number of blows during operation is recorded with depth of penetration. The slope of the relationship between number of blows and depth of penetration (in millimeters per blow) at a given linear depth segment is recorded as DCP penetration index (DPI).

Since DCP testing is basically a measure of penetration resistance, expressed as DCP penetration index (DPI), the analysis of the DCP data must be interpreted to generate a representative value of penetration per blow for the material being tested. This representative value can be obtained by averaging the DPI across the entire penetration depth at each test location. Two methods of calculating the representative DPI value for a given penetration depth of interest are: (i) arithmetic average and (ii) weighted average. [2] Since the weighted average method yielded narrower standard deviation for the representative DPI value and provided better correlations to other field tests than the arithmetic average method based on field data available. [2] Thus, the weighted average method was employed to calculate the representative DPI value in this study. The weighted average technique can be obtained as follows: [2]

$$DPI = \frac{1}{H} \sum_{i=1}^N [(DPI)_i \cdot (z)_i] \quad (2)$$

where  $z$  is the penetration distance per blow set and  $H$  is the overall penetration depth of interest. The DPI values are usually correlated with the California bearing ratio (CBR) of the pavement materials. In this study, the CBR obtained from the DCP will be defined as  $CBR_{DCP}$ . Extensive research [7-13] has been conducted to develop an empirical relationship between DPI and  $CBR_{DCP}$  for a wide range of pavement and subgrade materials and can be quantitatively presented in the form of:

$$\log(CBR_{DCP}) = \alpha + \beta \log(DPI) \quad (3)$$

where  $\alpha$  and  $\beta$  are coefficients ranging from 2.44 to 2.56 and -1.07 to -1.16, respectively, which are valid for a wide range of pavement and subgrade materials. Note also that  $CBR_{DCP}$  is in percent and DPI is in millimetres per blow (mm/blow). For a wide range of granular and cohesive materials, the US Army Corps of Engineers use the coefficients  $\alpha$  and  $\beta$  of 2.46 and -1.12, which have been also adopted by several agencies and researchers [14-17] and is therefore used in this study.

### 4. FIELD TESTING PROGRAM

In this study, a SSG and a DCP were used to measure the in-situ stiffness and strength index properties of the pavement materials, respectively. At least five SSG measurements and one DCP measurement were performed for one test location. The DCP was performed after the SSG but at the adjacent location of the SSG measurements.

The length of test section was approximately 100-200 m. The measurements were made at every 10 m depending on the length of test section. In this study, the measurements were made at three highway construction sites around the city of Bangkok, Thailand: Highway No. 35 Bangkok-Amphoe Pak Toe Section of Samutsakorn-Amphoe Pakto Part 4, Highway No. 351 Connection to Sukhapiban 1–Eastern Outer Ring Road, Keharomkroa Road development project. Three highway construction sites involved use of different unbound granular materials such as sand embankment, lateritic soil subbase, fine-grained aggregate subbase, and crushed rock base. The SSG and DCP were performed on these compacted pavement materials, which have been normally used in Thailand

highway construction. In addition, the Falling Weight Deflectometer (FWD) was performed on Highway No. 35 Bangkok-Amphoe Pak Toe Section of Samutsakorn-Amphoe Pakto Part 4. Due to the construction time constraint, the FWD was performed only on this highway.

## 5. MATERIAL CLASSIFICATION AND PROPERTIES

Samples were collected from three highway construction sites to determine index properties, soil classification, and compaction characteristics. A summary of the pavement materials encountered and their properties along with their classification are tabulated in Table 1. Note that in Thailand, the crushed rock base is subdivided into grade A, grade B, and grade C.

To compare the measured in-situ stiffness from the SSG and strength from the DCP, the laboratory resilient modulus and CBR of these pavement materials were also determined in this study. At least five replicated specimens for each test material were prepared at the 95% of maximum dry density near the optimum moisture content. An example of the resilient modulus of the crushed rock base grade C is illustrated in Figure 2. Results of the resilient modulus and CBR for all material tested are given in Table 2. Note that the resilient modulus and CBR tests were conducted according to AASHTO T309 and AASHTO T193, respectively.

**Table 1.** Properties of pavement materials and their classification

Material Classification and Properties	Sand Embankment	Lateritic Soil Subbase	Fine-grained Aggregate Subbase HWY 35	Fine-grained Aggregate Subbase HWY 351	Crushed Rock Base Grade C	Crushed Rock Base Grade A, B
AASHTO Classification	A-3	A-2-4	A-2-4	A-2-4	A-1-a	A-1-a
50.0 mm (1½")	100	100	100	100	100	100
25.0 mm (1")	100	97.7	100	99.7	100	98.9
19.0 mm (¾")	100	93.0	96.6	92.8	-	91.8
9.5 mm (3/8")	100	68.8	81.3	69.2	69.0	63.3
No. 4	98.5	40.1	63.8	53.6	47.0	42.1
No. 10	97.8	24.8	35.3	39.6	30.0	23.6
No. 40	93.6	16.4	19.6	23.3	18.0	10.5
No. 200	24.1	8.1	12.4	14.4	10.0	6.9
D <sub>10</sub> (mm)	0.055	0.1	0.051	0.02	0.86	0.29
D <sub>30</sub> (mm)	0.085	3.0	1.4	0.9	2.0	3.0
D <sub>60</sub> (mm)	0.18	7.3	4.1	7.0	7.5	9.0
LL (%)	N.P.	23.4	N.P.	N.P.	N.P.	N.P.
PI (%)	N.P.	7.6	N.P.	N.P.	N.P.	N.P.
O.M.C. (%)	9.5	6.5	5.4	6.5	5.7	6.0
γ <sub>dry, max</sub> (t/m <sup>3</sup> )	1.94	2.25	2.32	2.24	2.31	2.34

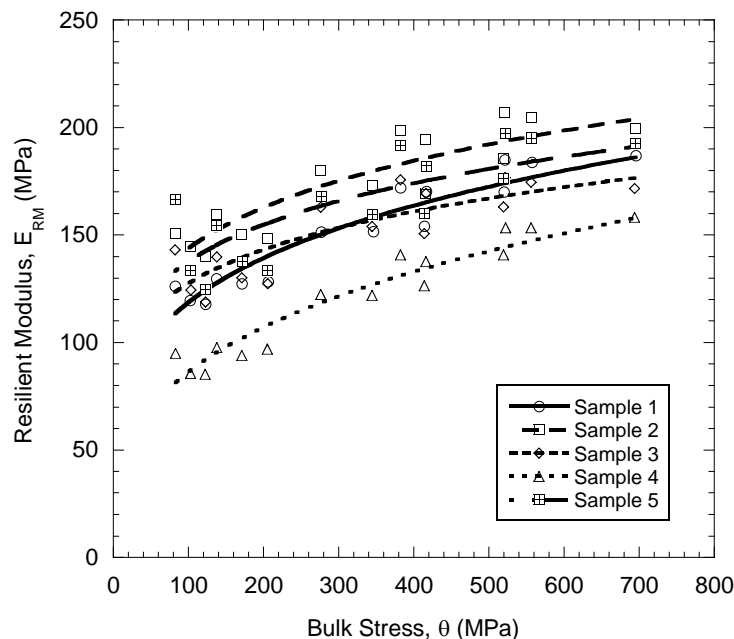


Figure 2. Resilient modulus and bulk stress ( $\theta = \sigma_1 + \sigma_2 + \sigma_3$ ) relationship for crushed rock base grade C.

## 6. RESULTS AND DISCUSSION

Statistical results of SSG and DCP measurements for all materials tested are presented in Figures 3 and 4. Each box encloses 50% of the data with the median value displayed as a line, the top and bottom of the box mark the limits of  $\pm 25\%$  of the data. The lines extending from the top and bottom of each box mark the minimum and maximum values within the data set that fall within an acceptable range. Any value outside of this range called an outlier is displayed as an individual point. The number of the data, the mean, and the standard deviation (SD) of each test materials were also given in the plot. In general, the stiffness of these unbound granular materials including crushed rock base, fine-grained aggregate subbase, and lateritic soil subbase fall within the same range (except for the fine-grained aggregate subbase from HWY No. 35) and are stiffer than the sand embankment. Among these unbound granular materials, the crushed rock base grade A and B have the highest mean stiffness, while the sand embankment has the lowest mean stiffness.

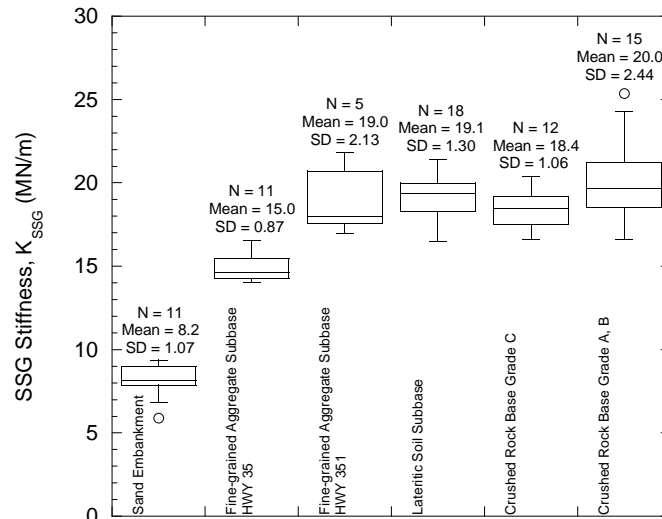


Figure 3. SSG stiffness ( $K_{SSG}$ ) of various pavement materials.

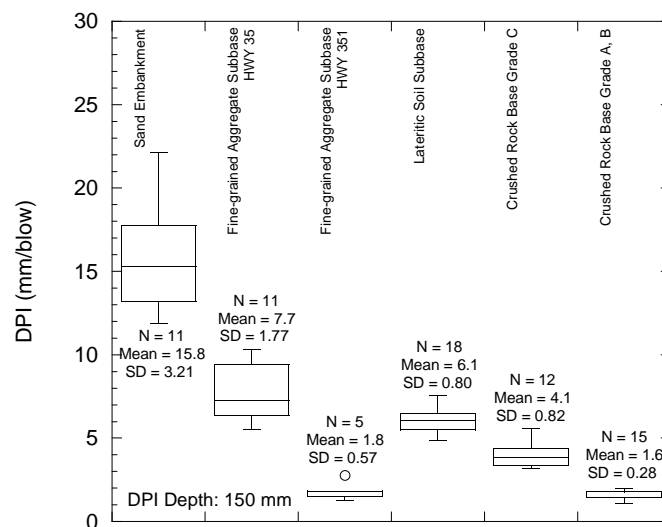


Figure 4. DCP penetration index (DPI) values of various pavement materials.

The DPI (amount of penetration per blow) is inversely proportional to shear strength of a material (i.e., the higher a DPI value, the lower a shear strength). The patterns exhibited by the DPI, in general, parallel those of  $K_{SSG}$  in Figure 3. Data in Figure 4 indicate that the standard deviation associated with DPI is smaller than that of  $K_{SSG}$  or crushed rock base, fine-grained aggregate subbase, and lateritic soil subbase. However in the case of sand embankment, the DPI gives larger standard deviation than  $K_{SSG}$ . This can be explained by the difference in measurement characteristics of each method.

The mean  $K_{SSG}$  and DPI were plotted against the mean diameter ( $D_{50}$ ) of the materials as shown in Figures 5 and 6, respectively. The mean  $K_{SSG}$  increased linearly with  $D_{50}$ , while the mean DPI decreased linearly with  $D_{50}$ . As expected, the materials with larger grain size tend to become stiffer and exhibit higher strength (lower DPI) than those with smaller grain size.

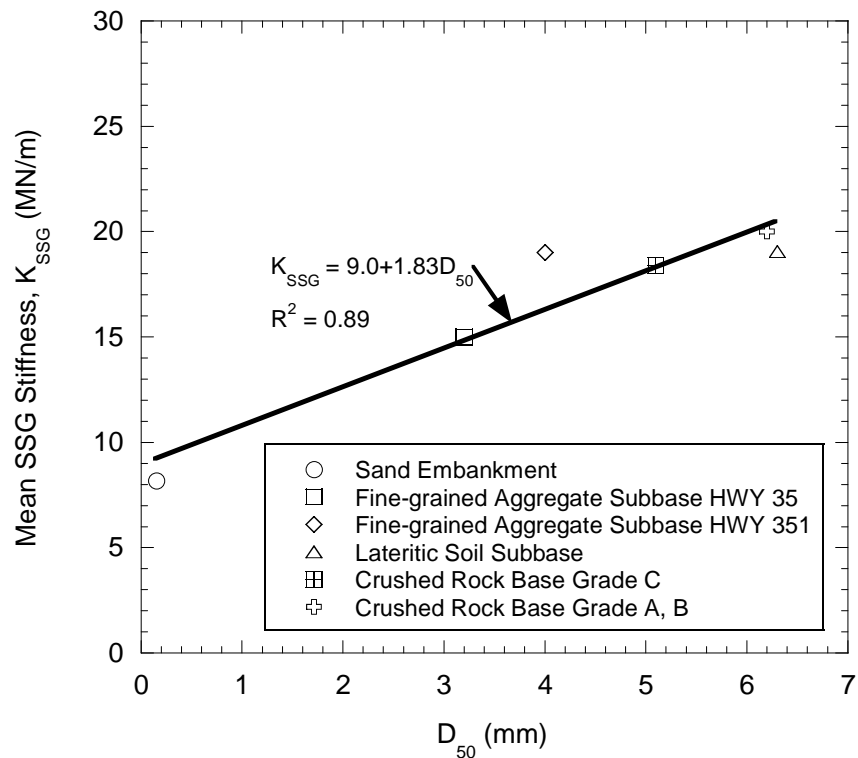


Figure 5. Mean  $K_{SSG}$  vs. mean diameter ( $D_{50}$ ) of various pavement materials.

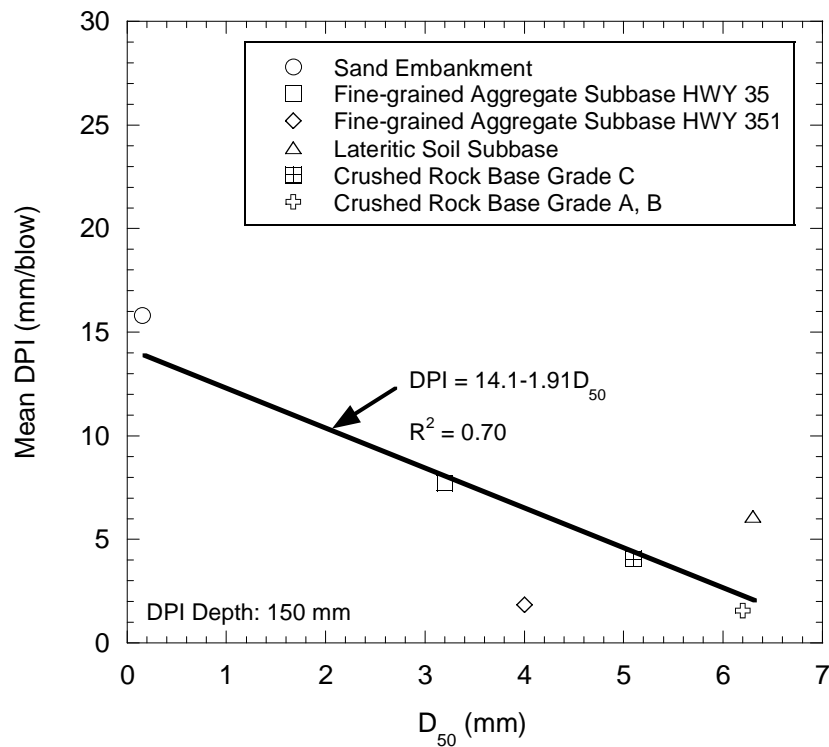


Figure 6. Mean DPI value vs. mean diameter ( $D_{50}$ ) of various pavement materials.

The correlation of  $K_{SSG}$  to DPI is examined based on four materials: (1) sand embankment, (2) fine-grained aggregate subbase, (3) lateritic soil subbase, and (4) crushed rock base. Figure 7 shows the relationship between  $K_{SSG}$  and log DPI for these materials.  $K_{SSG}$  is related to DPI in a simple linear semi-logarithmic relationship. Sawangsuriya and Edil [2] indicated that the linear regression was made between  $K_{SSG}$  and log DPI in the subgrade and subbase materials with the best correlations (i.e., highest  $R^2$ ) were obtained when DPI was averaged over a DCP penetration depth of 150 mm. Figure 8 illustrates the correlation between  $K_{SSG}$  and DPI obtained in this study combined with those reported in Sawangsuriya and Edil [2].  $K_{SSG}$  and DPI correlate well with a  $R^2$  of 0.81.

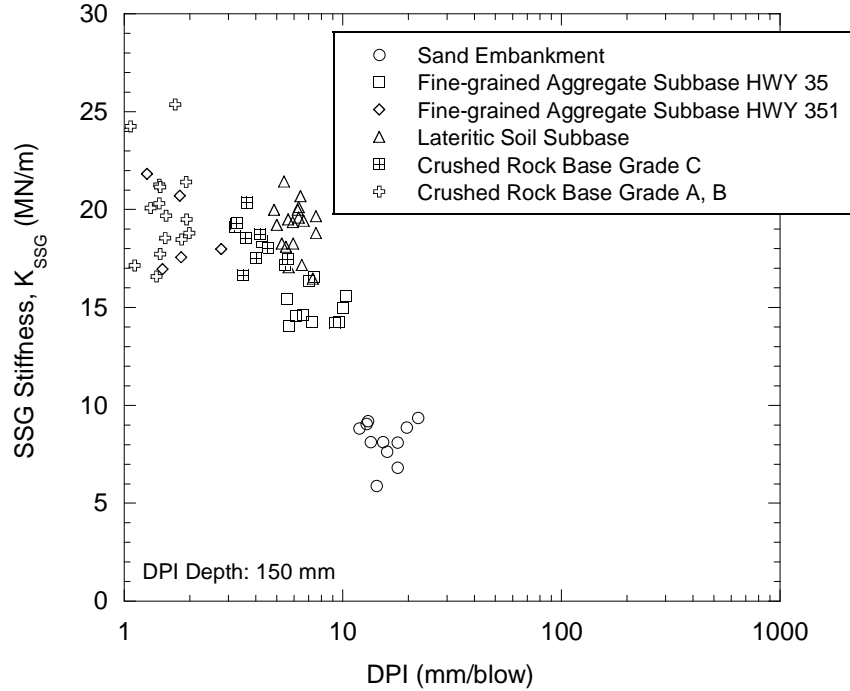


Figure 7.  $K_{SSG}$ -DPI relationship for various pavement materials.

After a simple linear semi-logarithmic relationship between  $K_{SSG}$  and DPI values was determined (i.e.,  $K_{SSG} = 24 - 10.8 \cdot \log \text{DPI}$ ) based on the direct regression from the actual measured data for all materials used in this study combined with data from Sawangsuriya and Edil [2] (Figure 8), such correlation can be further developed to become a more meaningful and useful equation, which can be used in the design of pavements. To accomplish that, the measured  $K_{SSG}$  is converted to SSG modulus ( $E_{SSG}$ ) of the pavement materials using Eq. (1). Values for Poisson's ratio ( $\nu$ ) of these unbound granular materials used in the study were assumed to be 0.30. Similarly, the weighted average DPI value obtained from the DCP can be converted to California bearing ratio ( $CBR_{DCP}$ ) of the pavement materials using the well-established correlation as given in Eq. (3) with the coefficients  $\alpha$  and  $\beta$  of 2.46 and -1.12, respectively. Figure 9 illustrates the plot of calculated  $E_{SSG}$  versus  $CBR_{DCP}$  for the materials used in the study. Similar to the  $K_{SSG}$ -DPI plot, the correlation data from Sawangsuriya and Edil [2] were combined with those obtained in this study. The regression equation obtained is expressed as follows:

$$E_{SSG} = -0.63 + 88.0 \log(CBR_{DCP}) \quad R^2 = 0.80 \quad (4)$$

where  $E_{SSG}$  and  $CBR_{DCP}$  units are in MPa and percent, respectively. It can be seen that a unique relationship exists between  $E_{SSG}$  and  $CBR_{DCP}$ , regardless of soil type and site. The results of SSG tests and DCP tests are expected to be affected by the same factors (i.e., relating both test results directly excludes the influence of water content, dry density, and other basic indices). The regression equation obtained in this study is also compared with the equation given by Powell et al. [18] (i.e.,  $E = 17.6 CBR^{0.64}$ ), AASHTO [19] (i.e.,  $E = 10 CBR$ ), and Sawangsuriya and Edil [2] (i.e.,  $E = 18.8 CBR_{DCP}^{0.63}$ ). This equation yields almost identical values to those obtained from the equations given by Powell et al., AASHTO, and Sawangsuriya and Edil for the CBR values < 10%. The suggested equation by AASHTO gives the highest modulus when the CBRs are greater than 10%. At relatively high CBRs (i.e., those of subbase and base materials), the equations given by Powell et al., AASHTO, and Sawangsuriya and Edil tend to overestimate the elastic modulus. Using Figure 10, elastic

modulus can be estimated for any pavement conditions if CBR is obtained for the corresponding condition.

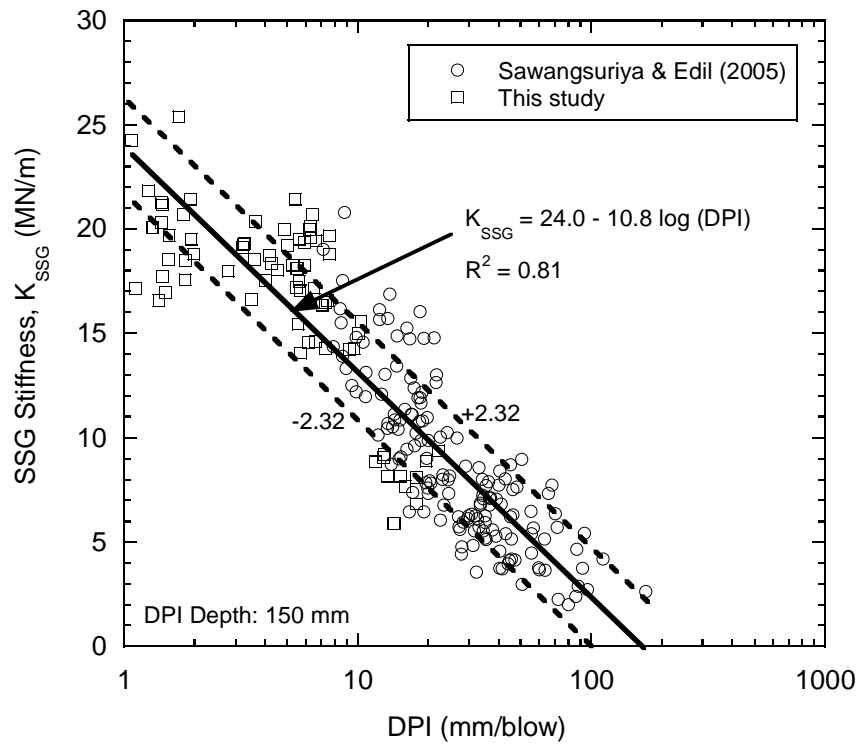


Figure 8. Linear semi-logarithmic relationship between  $K_{SSG}$  and DPI values.

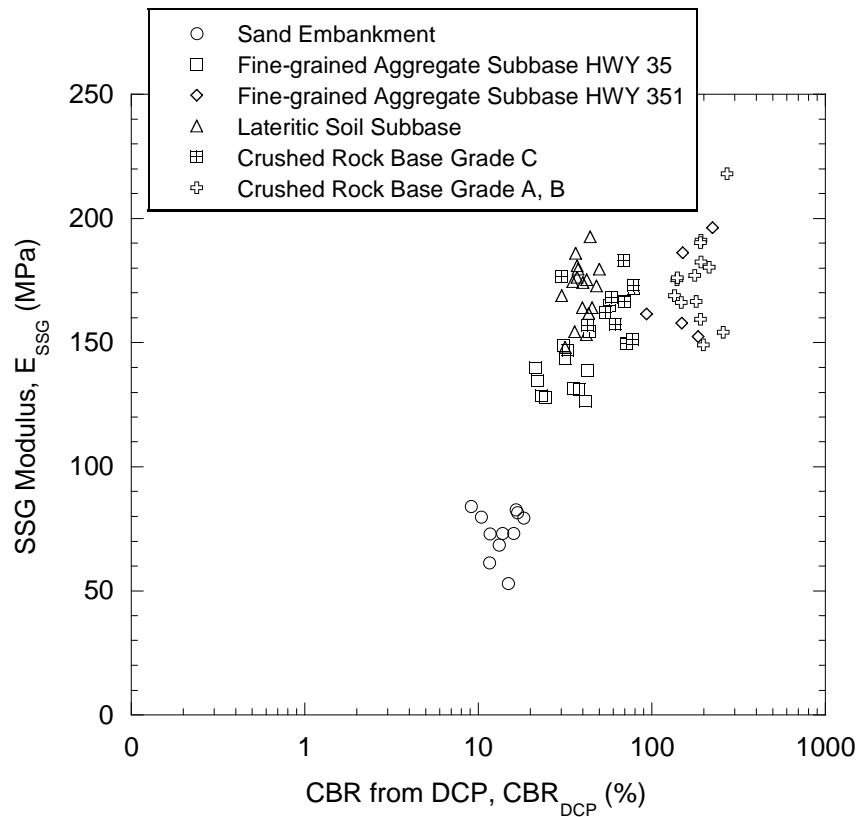


Figure 9.  $E_{SSG}$ - $CBR_{DCP}$  relationship for various pavement materials.



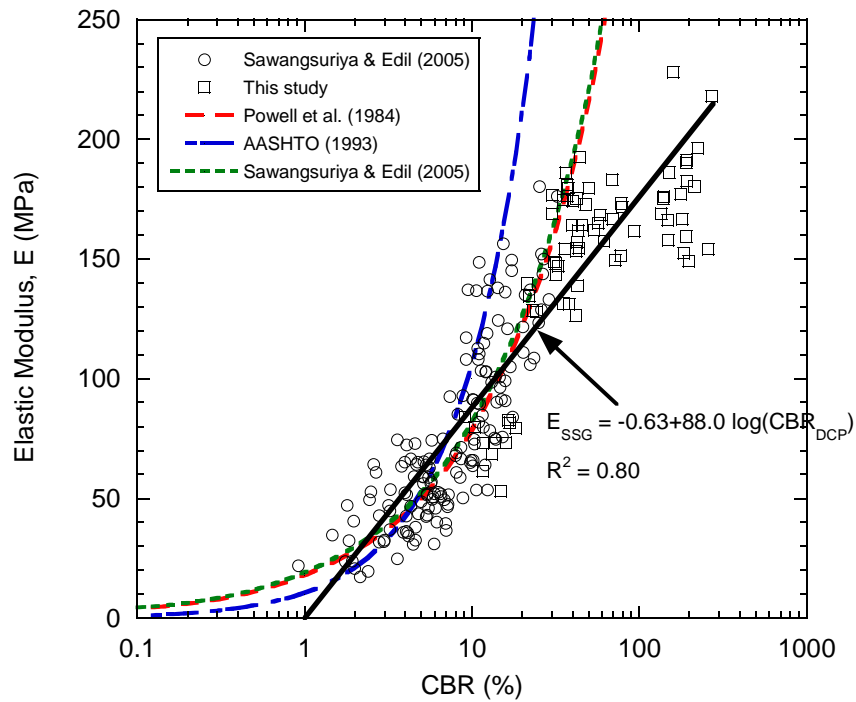


Figure 10. E-CBR relationship.

The elastic moduli obtained from the SSG ( $E_{SSG}$ ) were also compared with those obtained from the FWD ( $E_{FWD}$ ) and the resilient modulus test ( $E_{RM}$ ) as shown in Figure 11 and Table 2. In general,  $E_{SSG}$  tends to be smaller than  $E_{FWD}$  but agrees fairly well with  $E_{RM}$ . Similarly, the laboratory CBR ( $CBR_{Lab}$ ) falls in the range of the CBR from the DCP ( $CBR_{DCP}$ ) as presented in Table 2.

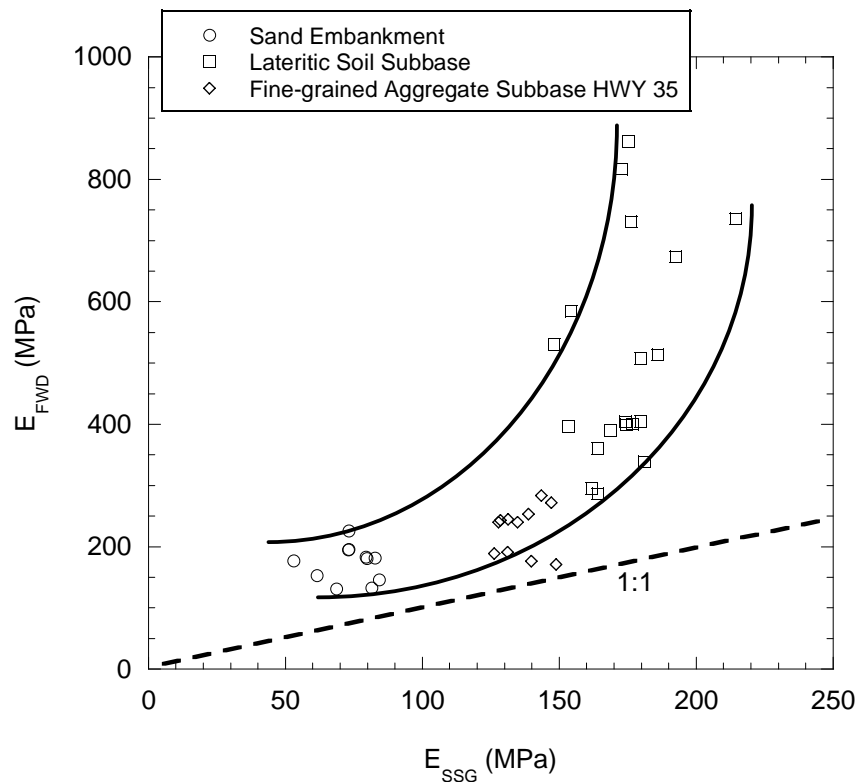


Figure 11. Comparison between moduli from the SSG and those from the FWD.

**Table 2.** Comparison with laboratory resilient modulus and CBR tests

Materials	$E_{SSG}$ (MPa)	$E_{RM}$ (MPa)	$CBR_{DCP}$ (%)	$CBR_{Lab}$ (%)
Sand Embankment	53 – 84	75 – 294	11 – 22	26
Lateritic Soil Subbase	148 – 240	180 – 230	31 – 52	27
Fine-grained Aggregate Subbase HWY 35	126 – 148	110 – 239	24 – 42	58
Fine-grained Aggregate Subbase HWY 351	152 – 196	118 – 285	91 – 218	58
Crushed Rock Base Grade C	149 – 183	80 – 203	46 – 95	83
Crushed Rock Base Grade A, B	149 – 228	119 – 290	135 – 272	105

## 7. CONCLUSIONS

SSG and DCP survey data of unbound granular materials from three highway construction sites around the city of Bangkok, Thailand are presented along with their correlation with each other. The SSG provides in-place near-surface soil stiffness, whereas DCP provides individual points of an index of in-situ shear strength expressed as DCP penetration index (DPI) as a function of depth. The weighted average of DPI over the depth of measurement is employed to obtain a representative strength index of the material. It is observed that the standard deviation associated with DPI is considerably smaller than that of the SSG stiffness.

A simple linear semi-logarithmic relationship is observed between SSG stiffness and DPI weighted average over a DCP penetration depth of 150 mm. Moreover, results of the regression analysis show that there is a significant correlation between the elastic modulus obtained from the SSG and the CBR obtained from the DCP. In this study, a linear semi-logarithmic model is developed between these two properties and is compared with equations suggested by Powell et al., AASHTO, and Sawangsuriya and Edil. The suggested equations tend to overestimate the pavement modulus for relatively high CBRs (i.e., those of subbase and base materials). The moduli from the SSG can be also correlated with the moduli from the FWD and the laboratory resilient modulus test. Similarly, the CBR from the DCP agrees fairly well with the laboratory CBR test.

The study indicates that both devices show good potential for future use in the pavement material evaluation. The in-situ stiffness and strength properties of various materials can be rapidly and directly monitored in companion with the conventional compaction control tests (i.e., nuclear density or laboratory moisture content samples) during earthwork construction. Direct monitoring of stiffness and strength of the pavement materials using these two devices appears to be effective in different phases of highway design, i.e., for long-term pavement performance as well as during construction quality control monitoring.

## REFERENCES

1. Nageshwar R., Varghese, G., and Shivashanka, R., PFWD, CBR and DCP Evaluation of Lateritic Subgrades of Dakshina Kannada, India, The 12th International Conference of International Association for Computer Methods and Advances in Geomechanics, Goa, India, 2008, pp. 4417-4423.
2. Sawangsuriya, A. and Edil, T. B., Evaluating Stiffness and Strength of Pavement Materials, Proceedings of the Institution of Civil Engineers-Geotechnical Engineering, 158, 4, 2005, pp. 217-230.
3. Briaud, J.-L., Li, Y., and Rhee, K., BCD: A Soil Modulus Device for Compaction Control, Journal of Geotechnical and Geoenvironmental Engineering, ASCE, 132, 1, 2006, pp. 108-115.
4. Sawangsuriya, A., Bosscher, P. J., and Edil, T. B., Laboratory Evaluation of the Soil Stiffness Gauge, Transportation Research Record 1808, TRB, National Research Council, Washington, D.C., 2002, pp. 30-37.

5. Sawangsuriya, A., Edil, T. B., and Bosscher, P. J., Relationship between Soil Stiffness Gauge Modulus and Other Test Moduli for Granular Soils, Transportation Research Record 1849, TRB, National Research Council, Washington, D.C., 2003, pp. 3-10.
6. Egorov, K. E., Calculation of Bed for Foundation with Ring Footing, Proceedings of the Sixth International Conference of Soil Mechanics and Foundation Engineering, 1965, 2, pp. 41-45.
7. Livneh, M., Ishao, I., and Livneh, N. A., Effect of Vertical Confinement on Dynamic Cone Penetrometer Strength Values in Pavement and Subgrade Evaluations, Transportation Research Record 1473, TRB, National Research Council, Washington, D.C., 1995, pp. 1-8.
8. Kleyn, E., Maree, J., and Savage, P., The Application of a Portable Pavement Dynamic Cone Penetrometer to Determine In Situ Bearing Properties of Road Pavement Layers and Subgrades in South Africa, Proceedings of the Second European Symposium of Penetration Testing, Amsterdam, 1982.
9. Harison, J. R., Correlation between California Bearing Ratio and Dynamic Cone Penetrometer Strength Measurement of Soils, Proceeding of Institute of Civil Engineers, Part 2, 1987, 83, Technical Note No. 463.
10. Livneh, M., Validation of Correlations between a Number of Penetration Tests and In Situ California Bearing Ratio Tests, Transportation Research Record 1219, TRB, National Research Council, Washington, D.C., 1987, pp. 56-67.
11. McElvaney, J. and Djatnika, B. I., Strength Evaluation of Lime-Stabilized Pavement Foundations Using the Dynamic Cone Penetrometer, Australian Road Research, 1991, 21, No. 1.
12. Webster, S. L., Grau, R. H., and Williams, T. P., Description and Application of Dual Mass Dynamic Cone Penetrometer, Instruction Report GL-92-3, U.S. Army Engineers Waterways Experimental Station, Vicksburg, MS, 1992, 17 pp.
13. Livneh, M. and Livneh, N. A., Subgrade Strength Evaluation with the Extended Dynamic Cone Penetrometer, Seventh International Association of Engineering Geologists Congress, ISBN 90 5410 503 8, 1994.
14. Konrad, J.-M. and Lachance, D., Use of In Situ Penetration Tests in Pavement Evaluation, Canadian Geotechnical Journal, 2001, 38, No. 5, pp. 924-935.
15. Webster, S. L., Grau, R. H., and Williams, T. P., Description and Application of Dual Mass Dynamic Cone Penetrometer, Instruction Report GL-92-3, U.S. Army Engineers Waterways Experimental Station, Vicksburg, MS, 1992, 17 pp.
16. Siekmeier, J. A., Young, D., and Beberg, D., Comparison of the Dynamic Cone Penetrometer with Other Tests during Subgrade and Granular Base Characterization in Minnesota, Nondestructive Testing of Pavements and Back Calculation of Moduli, ASTM STP 1375, West Conshohocken, PA, 1999.
17. Chen, D.-H., Wang, J.-N., and Bilyeu, J., Application of the Dynamic Cone Penetrometer in Evaluation of Base and Subgrade Layers, Transportation Research Record 1764, TRB, National Research Council, Washington, D.C., 2001, pp. 1-10.
18. Powell, W. D., Potter, J. F., Mayhew, H. C., and Nunn, M. E., The Structural Design of Bituminous Roads, TRRL Laboratory Report 1132, Transportation and Road Research Laboratory, Crowthorne, Berkshire, 1984, 62 pp.
19. AASHTO, Guide for Design of Pavement Structures, American Association of State Highway and Transportation Officials, Washington, D.C., 1993.